IOP Conf. Series: Materials Science and Engineering **281** (2017) 012051 doi:10.1088/1757-899X/281/1/012051

# Simulation of Ion Energy Distributions in ICP Reactor with Bias Voltages Using COMSOL

**C K Han[1], Y Y Yang[1*], W F Liu[1], J Cheng[2], Y J Lu[2] and L H Ji[2]**

[1] School of Engineering and Technology, China University of Geosciences (Beijing), Beijing 100083, China
[2] Department of Mechanical Engineering, Tsinghua University, Beijing 100084, China

E-mail: yangyy@cugb.edu.cn

**Abstract.** An inductively coupled plasma reactor driven by continuous wave (cw) or pulse source with dc bias is introduced to investigate the plasma parameters and ion energy distributions using COMSOL and compared with experimental results. The results show that with the increase of pressure, the electron density varies from $4.5\times10^{11}cm^{-3}$ to $16.7\times10^{11}cm^{-3}$, and electron temperature is in the range of 3.3eV to 3.9eV. For pulsed power, the change of electron temperature is corresponding to the duty cycle of pulse power. With the dc bias, the ion energy peaks shift from 8eV to 19.5eV, and the full width at half maximum (FWHM) of the IEDs varies in the range of 0.5eV to 2.7eV. Finally, application of a synchronous dc bias in the afterglow of pulsed plasma leads to a bi-modal IEDs with a sharper peaks at lower energy during the afterglow and a broader peak at higher energy when the power is on.

## 1. Introduction

The control of ion energy bombarding the wafer is important in anisotropic plasma etching and deposition process [1, 2]. With the decrease of line width and increase in the scale of wafer, precise and independent control of the ion energy distribution (IEDs) and fluxes which determine selectivity of plasma etching and etch rate becomes critically important [3, 4]. Many methods have been developed to control the plasma parameters and IEDs independently [5], such as dual-frequency capacitively coupled plasma source (DF-CCPs), inductively coupled plasma source (ICPs) with bias voltage and pulsed plasma source with synchronous bias voltage, et al. Due to the high density of plasma and the independent control of ion energy distributions, ICPs with bias voltages have been widely used in integrated circuit manufacture, especially deposition and etching process. In ICPs with bias voltage system, the coil power intends to generate and sustain plasma while bias power intends to control IEDs and ion fluxes.

To date, there are many the researches of investigating and controlling the structure of IEDs using analytical methods, experimental measurement and simulation models. The retarding field energy analyser (RFEA) has been introduced to investigated the IEDs for both rf-biased and moderating the shape of bias voltage waveform ICPs or CCPs in argon and helicon plasma [6-10]. The influence of discharge pressure, bias power and coil power on the IEDs and ion angle distributions (IADs) are investigated in the studies. An extended semi-analytic collisionless sheath model is used to obtained the IEDs and IADs for muti-frequency CCPs [11]. Hybrid fluid model and PIC/MCC model are introduced to analyse the plasma parameters and IEDs in both ICP and CCP discharge for Ar, $CF_4$ and

$O_2$ [12-16]. The influence of bias frequency, discharge pressure, voltage amplitude, gas species and bias power on the plasma parameters and IEDs are simulated. However, the pulsed ICP discharge with dc bias, which is used in industrial manufacture, has been rarely investigated by simulation method. In this paper, both cw and pulsed source power ICP argon discharge with dc bias is investigated by COMSOL under variety of discharge condition. The plasma parameters and IEDs are obtained under various discharge condition. The control of IEDs using inductively coupled pulsed plasma with dc bias is investigated.

## 2. Model description

A 2D axisymmetric schematic diagram of the ICP reactor used in this work is given in Figure1 [6]. Plasma is sustained in an 80 mm diameter dielectric tube with a three-turn spiral coil (10 mm sider length) around quartz window (the relative permittivity sets to 4.2). In this study, plasma source can be selected between cw powers at 13.56 MHz and pulsed at 10 KHz power. The input nozzle is placed at the top of chamber, which consists of three nested metal cylinders 30 mm tall and 13, 32 and 40 mm in radius (the electrical conductivity is set to $10.2\times10^6$ S/m ). The walls of inner chamber except the symmetry axis and electrode are all grounded. The interfaces between plasma and quartz tube are dielectric (surface charge accumulation is used here). External boundaries of system except the symmetry axis are magnetically insulated ($n\times\mathbf{A}=0$, n is the surface normal and **A** is the magnetic vector potential). The air case surrounding the coils is considered to vacuum characteristics.

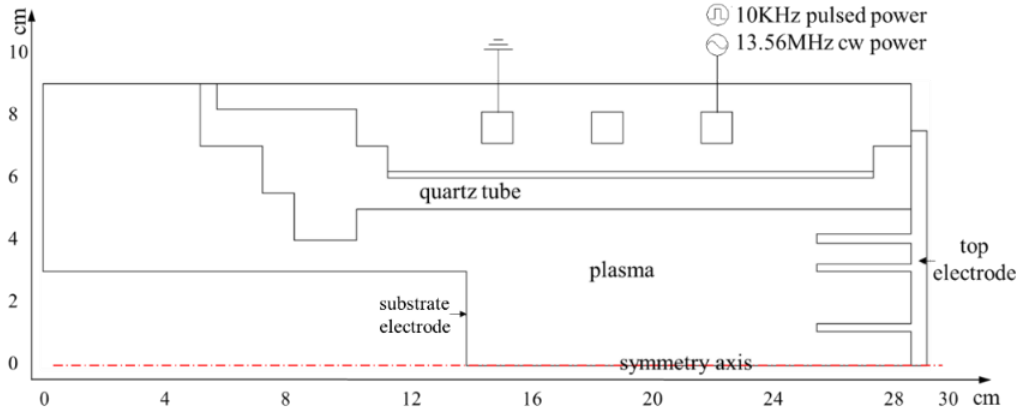


**Figure 1.** The schematic diagram of the ICP reactor

The main collision parameters of argon gas used in this simulation are listed in table 1:

**Table 1**. The main collision parameters in the argon discharge [17].

| Formula | Collision | Energy loss (eV) |
|---|---|---|
| e+Ar=>e+Ar | Elastic | -- |
| e+Ar=>e+Ar* | Excitation | 11.5 |
| e+Ar*=>e+Ar | Super elastic | -11.5 |
| e+Ar=>2e+Ar+ | Ionization | 15.8 |
| e+Ar*=>2e+Ar+ | Ionization | 4.24 |
| Ar*+Ar*=>e+Ar+Ar+ | Penning Ionization | -- |
| Ar*+Ar=>Ar+Ar | Metastable quenching | -- |

In table 1 the symbols + and * denote positive ions and metastable atoms respectively.

## 3. The ORY description

The plasma module in COMSOL is based on fluid model [18-20]. In this study, the electron energy distribution function (EEDF) is assumed to Maxwellian. Since the discharges are operated at low

pressure (up to 50 mTorr) and the electron energy is low (up to 6 eV), the assumption is appropriate in this study [21]. Monte Carlo (MC) model is applied to capture ions trajectories until they collide with the wafer surface [22].

*3.1. Fluid module*

The spatio-temporal distributions of particles and the electric field are obtained by solving the coupled Maxwell equations, continuity equations of electron, energy balance equation of electron, continuity equations of ions and Poisson's equation as follows [19],

$$\frac{\partial n_e}{\partial t} + \nabla \cdot \mathbf{\Gamma}_e = \mathrm{R_e} - (u \cdot \nabla) n_e ; \mathbf{\Gamma}_e = -\left(\mu_e \cdot \mathbf{E}\right) n_e - D_e \cdot \nabla n_e \tag{1}$$

$$\frac{\partial n_\varepsilon}{\partial t} + \nabla \cdot \mathbf{\Gamma}_\varepsilon + \mathbf{E} \times \mathbf{\Gamma}_e = R_\varepsilon - (\mathbf{u} \cdot \nabla) n_\varepsilon + \frac{Q}{q}; \mathbf{\Gamma}_\varepsilon = -\frac{5}{3}((\mu_e \cdot \mathbf{E}) n_e + D_e \cdot \nabla n_e)\varepsilon - \frac{5}{3}(D_e \cdot \nabla \varepsilon) n_e \tag{2}$$

$$\rho \frac{\partial w_k}{\partial t} + \rho(\mathbf{u} \cdot \nabla) w_k = \nabla \cdot \mathbf{j}_k + R_k \tag{3}$$

where parameters undefined are listed in table 2.

**Table 2.** The undefined parameters in the fluid model

| | |
|---|---|
| $n_e$ — the electron number density | $\mathbf{\Gamma}_e$ — the electron flux vector |
| $R_e$ — source or sink of electrons | **u** — the averaged mass fluid velocity vector |
| $n_\varepsilon$ — the electron energy density | $\mathbf{\Gamma}_\varepsilon$ — the electron energy flux vector |
| $\mu_e$— the electron mobility | $D_e$— the electron diffusivity |
| $R_\varepsilon$ — the energy loss by inelastic collision | Q — the external power |
| q — the charge of an electron | **E** — the electric field intensity |
| ρ — the mixture gas density | $w_k$ — the mass fraction of the *k*th species |
| **u** — the averaged mass fluid velocity vector | $\mathbf{j}_k$— the diffusive flux vector |
| $R_k$— velocity rate of the *k*th species | |

*3.2. Electromagnetic module*

For a non-polarized plasma, a frequency domain Maxwell equations are applied to compute the electromagnetic distribution of the charge system. The magnetic vector potential **A** as the independent variable is computed in the frequency domain using the following Eq. (4) and (5),

$$(j\omega\sigma - \omega^2 \varepsilon_0 \varepsilon_r)\mathbf{A} + \nabla \times (\mu_0^{-1} \mu_r^{-1} \nabla \times \mathbf{A}) = \mathbf{J}_e \tag{4}$$

$$-\varepsilon_0 \nabla^2 V = \rho \tag{5}$$

where parameters undefined are listed in table 3.

**Table 3**. The undefined parameters in the electromagnetic model

| | |
|---|---|
| ω — the angular frequency of power source | $\mathbf{J_e}$ — the external current |
| σ — electrical conductivity of the system | $\varepsilon_0$ — the vacuum permittivity |
| $\varepsilon_r$ — relative permittivity of the system | $\mu_0$ — the vacuum permeability |
| $\mu_r$ — relative permeability of the system | V — the electric potential |

*3.3. MC module*

The charge particle tracing (CPT) module based on MC model is applied in this work [22]. The ion speed reduces to zero after collision with wafer to ensure the ion energy is captured only once. The ion energy distribution on the wafer is calculated in this model.

The distribution equation is defined by Eq. (6),

$$f(v_i) = \sqrt{\frac{M}{2\pi kT}} \exp\left(-Mv_i^2/2kT\right) \tag{6}$$

where M is ion mass, k is the Boltzmann coefficient, T is the initial temperature of ions which is 300K in this work, $v_i$ is the ion velocity.
The collision probability is defined by Eq. (7),

$$P = 1 - \exp(-\nu\Delta t) \tag{7}$$

where ν is the collision frequency between ions and neutral particles, Δt is the time step .

## 4. Results and description

Compared with experimental results from [6], the plasma parameters are discussed in this paper. The discharge conditions are: an initial gas temperature of 300K, a coil power of 300W and initial electron energy of 3eV.

### *4.1. Discharge with pulsed source power*

Figure 2 shows the electron number density along the chamber symmetrical axis under different pressures when the bias electrode is grounded. As shown in Figure 2, the electron number density ($n_e$) is higher in the central chamber than the electrode due to the diffusion and recombination of ions and electrons at the electrode and wall. The $n_e$ increases from $4.5\times10^{11}$ $cm^{-3}$ to $16.7\times10^{11}$ $cm^{-3}$ with the increase of discharge pressure. The result shows that the variation of electron number density is in good agreement with the experimental results, especially for 14mTorr discharge. Because of the Maxwellian EEDF assumption and simplification of electron transport coefficient by Einstein's equation, the peak density position (215mm) in this work is smaller than experimental results (230mm). In addition, the electron density next to electrode is much higher than experimental results (the $n_e$ is $11.2\times10^{11}$ $cm^{-3}$ in simulation and $2\times10^{11}$ $cm^{-3}$ in experiment at 170mm for 50mTorr). Because the fluid model used in this study does not consider the sheath region, the gradient of electron density adjacent boundary becomes smaller, resulting in a higher electron number density. Meanwhile, a quasi-neutral hypothesis is applied to the whole chamber.

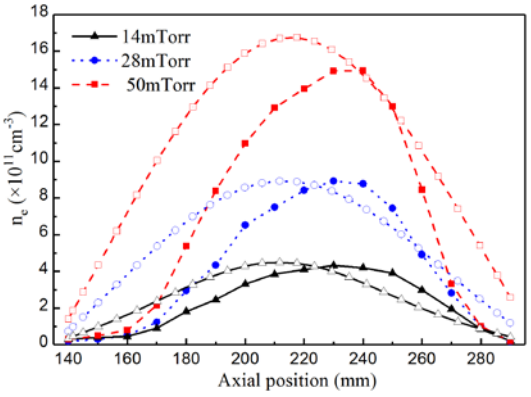


**Figure 2**. Electron number density plots as a function of symmetrical axis with cw power for different discharge pressures. The hollow icon is simulated results, the solid icon is experimental results from [6].

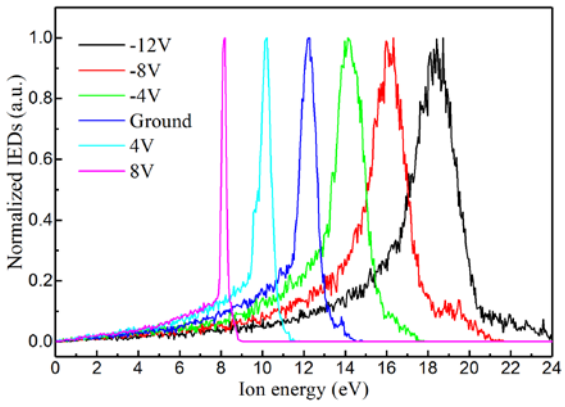


**Figure 3**. Normalized IEDs plots as a function of dc bias voltages applied to the bias electrode with cw source power.

Figure 3 demonstrates the normalized IEDs under different dc bias voltages applied to the substrate electrode. The bias voltage applied to the substrate electrode will shift the peak of ion energy. The dc

bias voltages have influence on the FWHM of IEDs. When positive voltages are applied, ions may not reach the wafer due to the suppression of bias electric field. Since ion energy lower than the threshold energy can't be captured, the ion energy broadening will be narrower. The offset of IEDs peak is proportional to the increase of bias voltage. Bias voltages applied to the substrate electrode affect the damped potential which directly determine the movement of ion transits the plasma sheath region. Because of a more directly influence on the damped potential, the peak of ion energy has a larger offset and the energy broadening can become narrower when bias voltage is applied to the substrate electrode.

*4.2. Discharge with pulsed source power*

To obtain nearly menoenergetic IEDs, narrowing the ion energy broadening which can be achieved by lowering electron temperature can be efficient. Pulsed plasma power can reduce electron temperature and maintain a constant sheath damped voltage. With a dc bias voltage applied to the substrate electrode, a narrower broadening IEDs will be achieved.

Figure 4 and Figure 5 show the electron density and electron temperature under different pressures and power duty ratios. The results show that the ne is increase from $4.75\times10^{10}$ $cm^{-3}$ to $3.7\times10^{11}$ $cm^{-3}$ with the increase of discharge pressure, the peak density position decreases to 195mm. Electron temperature increases rapidly after the plasma source turns on, overshoots then decreases to a steady value. Since electrons obtain energy from power source, electron energy increases sharply and presents rapid increase in electron temperature. Because of the collision between electron and other particles, electron energy consuming in excitation and ionization process cause the decrease of electron temperature. As expected, electron temperature decreases with increasing pressures due to the increase of collision probability between electron and other particles. After the plasma source turns off, electron temperature decreases rapidly and then reaches steady in the afterglow. Meanwhile, electron temperature decreases faster in low pressure because of a faster diffusion rate which determines the cooling mechanism at low pressure.

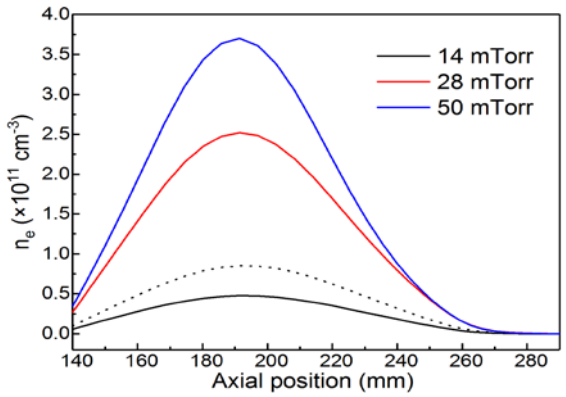


**Figure 4.** Electron number density plots as a function of symmetrical axis with pulsed power for different duty ratios and discharge pressure, with 120W time averaged power. Solid line is cycle of 20%, dot line is cycle of 50% duty ratio at 14 mTorr.

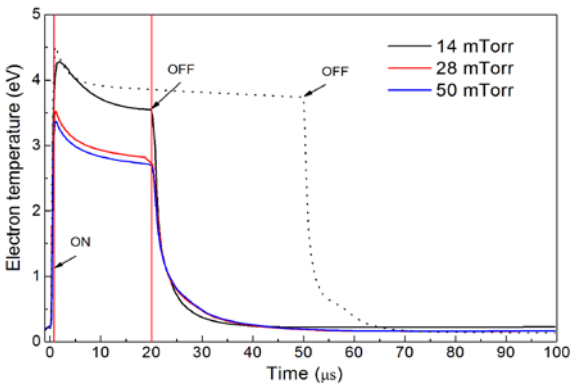


**Figure 5.** Electron temperature plots in a cycle for pulsed plasma in10KHz for different duty ratios and discharge pressure, with 120W time averaged power. Solid line is cycle of 20%, dot line is cycle of 50% duty ratio at 14 mTorr.

Figure 6 shows the normalized IEDs for pulsed source power coupled with dc bias voltage applied to bias electrode. With the decrease of dc voltage, the structure of IEDs transforms from uni-modal towards bi-modal with higher low energy peaks and broad high energy peaks. Because the dc bias directly affect sheath damped potential, the structure of IEDs will be changed in cycle of source power. When bimodal IEDs is obtained, the low energy peaks vary in the range of 4.2 to 12.2 eV, which is corresponding to the amplitude of bias voltage. The broader energy peak is corresponding to the condition when plasma source turns on. The narrower and higher energy peak is correspond to the

afterglow of pulsed plasma condition. The sheath potential is equal to the bias voltage when plasma source turns off, ions accelerated by bias electric field results a sharper peak in low energy.

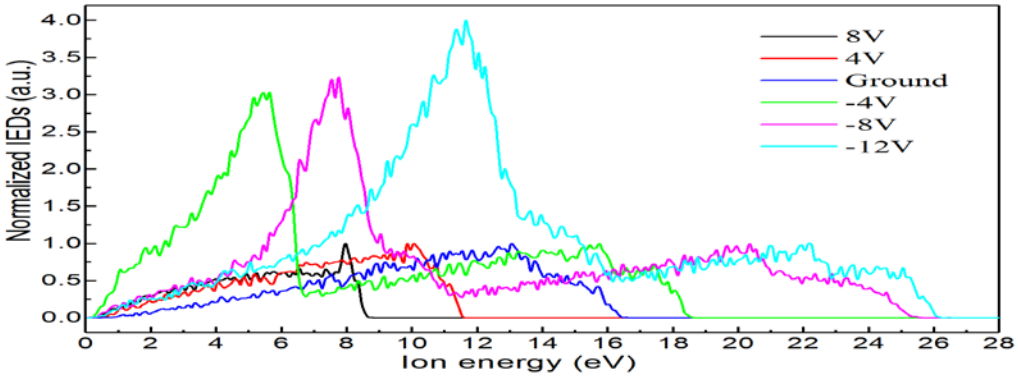


**Figure 6.** Normalized IEDs obtained under pulsed power with different dc bias voltage applied to the substrate electrode.

## 5. Conclusions

In this paper, dc bias ICP argon discharge driven by cw/pulsed source power is simulated and discussed by COMSOL. Both cw power and pulsed power source with dc bias voltage are investigated. The results indicate that the electron density is proportional to the discharge pressure. With the increase of discharge pressure, the electron density increases accordingly. Secondly, bias voltage has a strong influence on IEDs. Bias voltages can shift ion energy peak and affect the peak energy broadening. Finally, pulsed plasma discharge with dc bias voltage is investigated. A periodic change in plasma parameters and bimodal IEDs are found in a discharge cycle. Furthermore, a broad peak corresponds to ion energy during plasma on phase, while the sharper peak corresponds to the dc bias voltage during plasma off. Because of the Maxwellian EEDF assumption, there are some errors in the density peak position (it is at 215mm for cw power and 195mm for pulse power in simulation, which is 230 mm in experimental results). The electron transport coefficients calculated by Einstein equation cause error in electron potential which finally generates larger deviation in IEDs. In the future, EEDF obtained by experimental results or calculated by electron Monte-Carlo simulation model (EMCSM) will be coupled with fluid model.

## Acknowledgement

This study is financially supported by the China Important National Science and Technology Specific Project No. 2 (2011ZX02403-004).

## References

[1] Greene W M, Hartney M A, Oldham W G and Hess D W **1988** *J. Appl. Phys. 63* 1367
[2] Chen W C and Pu Y K **2014** *J. Phys. D:* Appl. *Phys. 47* 345201
[3] Economou D J **2013** *J. Vac. Sci. Technol., A. 31* 050823
[4] Agarwal A, Stout P J, Banna, S, Rauf S, Tokashiki K and Lee J Y **2009** *J. Appl. Phys. 106* 103305
[5] Lieberman, M A and Lichtenberg, A J **2005** *Principles of Plasma Discharges and Materials Processing*, 2nd ed. Wiley, New York p 351
[6] Shin H, Zhu W, Xu L, Donnelly V M and Economou D J **2011** *Plasma Sources Sci. Technol.20* 055001
[7] Wang S B and Wendt A E **2000** *J. Appl. Phys. 88* 643
[8] Woodworth J R, Riley M E, Miller P A, Hebner G A and Hamilton T W **1997** *J. Appl. Phys. 80* 1304
[9] Qin X V, Ting Y H and Wendt A E **2010** *Plasma Sources Sci. Technol. 19* 065014
[10] Ye C, He H, Huang F, Liu Y and Wang X **2014** *Phys. Plasmas. 21* 043509

[11] Kwon D C, Song M Y and Yoon J S **2013** *J. Phys. D: Appl. Phys.46* 025202
[12] Wang D, Ma T C and Deng X D **1973** *J. Appl. Phys. 74* 2986
[13] Zhang Y T, Kushner M J, Sriraman S, Marakhtanov A and Holland J **2015** *J. Vac. Sci. Technol., A. 33* 031302
[14] Dai Z L, Yue G and Wang Y N **2012** *Plasma Sci. Technol. 14* 240
[15] Kawamura E, Lieberman M A and Graves D B **2014** *Plasma Sources Sci. Technol. 23* 064003
[16] Zhang Y T, Kushner M J and Shannon S **2015** *J. Appl. Phys. 117* 233302
[17] https://fr.lxcat.net/home/
[18] COMSOL 4.4, Userbook
[19] Hagelaar G J and Pitchford L C **2005** *Plasma Sources Sci. Technol. 14* 722
[20] Key R J, Coltrin M E and Glarborg P **2003** *Chemically Reacting Flow Theory and Practice.* Wiley, New York
[21] Panagopoulos T, Kim D, Midha V and Economou D J **2002** *J. Appl. Phys. 91* 2687
[22] Boffard J B, Jung R O, Lin C, Aneskavich L E and Wendt A E **2011** *Plasma Sources Sci. Technol. 20* 055006